Alexandria Journal of Medicine (2017) **53**, 123–133

HOSTED BY

Alexandria University Faculty of Medicine

Alexandria Journal of Medicine

http://www.elsevier.com/locate/ajme

Histological changes of the adult albino rats entorhinal cortex under the effect of tramadol administration: Histological and morphometric study

Ibrahim K. Ragab [a,*], **Hala Z.E. Mohamed** [b]

[a] *Histology Department, Faculty of Medicine, AL-Azhar University in Assiut, Egypt*
[b] *Human Anatomy and Embryology Department, Faculty of Medicine, Assiut University, Egypt*

Received 3 February 2016; revised 13 April 2016; accepted 6 May 2016
Available online 3 June 2016

KEYWORDS

Tramadol;
Entorhinal cortex;
Rats

Abstract *Background:* Tramadol is a centrally acting synthetic analgesic agent with opioid activity. Tramadol is used to treat moderate to severe pain. The entorhinal cortex has initially attracted attention because of its strong reciprocal connections with the hippocampal formation and its involvement in certain brain disorders.
Aim of work: The present study was designed to assess the deleterious effects of tramadol on the entorhinal cortex of the adult male albino rats.
Materials and methods: The study was carried out on 40 adult male rats. The rats were divided equally into two groups: control group, received 1 ml normal saline 0.9% intraperitoneally for 4 weeks. Treated group received 50 mg/kg/day of tramadol intraperitoneally for 4 weeks. All animals were anaesthetized by ether inhalation and perfused by normal saline. The brains were extracted from the skulls. For light microscopy, the brains of 10 animals in each group were processed for paraffin sections and stained by Gallocyanine stain. For electron microscopy, the entorhinal cortex was dissected in 10 brains of each group and processed. Semithin sections were prepared and stained with toluidine blue. Morphometric and statistical studies were performed.
Results: By light microscopy, the treated groups showed neuronal cells disorganization. Apoptotic cells were detected. In addition, diffuse chromatolysis of nuclear chromatin, absence of nucleoli, multinuclear cells, intercellular edema and a congested blood capillary were noticed. By electron microscopy, the treated groups of both lateral and medial entorhinal areas showed granular and pyramidal apoptotic cells. The morphometric and statistical studies showed significant increase of apoptotic index % in treated group as compared with control group.

* Correspondence to: Ibrahim K. Ragab, MD Department of Histology, Faculty of Medicine, Al-Azhar University, Assiut, Egypt. Tel.: +035378519; 01143592374; fax: +0882180445.
E-mail address: ibrahim_ragab12@hotmail.com (I.K. Ragab).

Peer review under responsibility of Alexandria University Faculty of Medicine.

http://dx.doi.org/10.1016/j.ajme.2016.05.001

Conclusion: Tramadol had degenerative effects on both lateral and medial entorhinal areas. Light as well as electron microscopic examination of entorhinal areas came to prove these effects. Tramadol abuse should be avoided without medical description due to its toxic effects.

1. Introduction

Tramadol is listed in many medical guidelines for pain treatment and the WHO guidelines for cancer pain relief mentioned it as a step-2 analgesic.[1] In chronic non-cancer pain, tramadol may be appropriate when non-opioid analgesics are ineffective or contraindicated. Tramadol is used to treat different degrees of pain ranging from moderate to severe pain.[2–4]

Tramadol is a centrally acting synthetic analgesic agent with opioid activity. It is known to provide pain relief by means of its primary metabolite, *O*-desmethyltramadol.[5,6] Its withdrawal reactions include restlessness, agitation, anxiety, sweating, insomnia, hyperkinesia, tremor, paresthesias and gastrointestinal symptoms; similar to opioid withdrawal symptoms.[7,8] Sustained-release preparations show a better tolerability profile.[3]

Compared to the classical opioid analgesic morphine, tramadol is considered to be a relatively safe analgesic. Few cases of fatal poisoning due to tramadol alone have been reported in the literature.[9–11] More frequent are intoxications with co-ingestion of other drugs or alcohol.[12,13] Symptoms following tramadol intoxication are similar to those of other opioids analgesics. These include central nervous system depression, coma, nausea and vomiting, tachycardia, cardiovascular collapse, seizures and respiratory depression up to respiratory arrest. Moreover, in combination with serotonergic agents (in particular, selective serotonin reuptake inhibitors and monoamine oxidase inhibitors) tramadol may induce the serotonin syndrome.[14–16]

Animal studies did not reveal a carcinogenic effect of tramadol. In addition, mutagenicity studies did not show evidence of a genotoxic risk to human. Studies on the sub-acute and chronic toxicity of tramadol have been carried out in rats, dogs and rabbits. Tramadol was administered orally, subcutaneously, intravenously, intramuscularly and rectally.[17]

The entorhinal cortex (EC) (ento = interior, rhino = nose, entorhinal = interior to the rhinal sulcus) is part of the medial temporal lobe or hippocampal memory system and constitutes the major gateway between the hippocampal formation and the neocortex. The entorhinal cortex has initially attracted attention because of its strong reciprocal connections with the hippocampal formation and its involvement in certain brain disorders.[18] It is divided into medial and lateral regions. Neurons in the entorhinal cortex are grouped into different layers that are characterized by a dominant cell type. Six layers are commonly distinguished, of which layers I and IV (lamina dissecans) are relatively free of neurons. The principal neurons of the entorhinal cortex, i.e., the neurons that are among the main recipients of incoming axons and constitute the major source of entorhinal output to a variety of cortical and subcortical structures, are generally pyramidal cells or modified versions, the so-called stellate cells.[19,20]

Severe alteration of the entorhinal cortex is associated with several disorders of the human brain, importantly Alzheimer's disease, temporal lobe epilepsy and schizophrenia.[21,22] Entorhinal atrophy is associated with mild memory loss as seen in individuals with mild cognitive impairment. Temporal lobe epilepsy is associated with marked degeneration in layer III of entorhinal cortex.[23,24]

So, this study aimed to assess the deleterious effects of tramadol on the entorhinal cortex of the adult male albino rats using histological and morphometric study.

2. Materials and methods

2.1. Drug

Tramal [Tramadol HCl, 50 mg capsules, Mina-Pharm, Egypt] was obtained from Pharmacology department, Faculty of Medicine, Assiut University. Tramadol hydrochloride is an odorless, white to off-white crystalline powder that is readily soluble in both water and ethanol.

2.2. Experimental animals

The study was carried out on 40 adult male Sprague-Dawley rats, weighing on average 180–200 g. These animals were housed in the animal house of Assiut University in cages containing bedding of fine wood which was changed twice weekly. They were maintained under light dark cycle (12/12) hours, at a (25 ± 5) °C. All rats were fed standard rat chow before starting the experiment. The standard rat chow diet (AIN-93M diet formulated for adult rodents) was prepared according to the National Research Council (NRC) 1978.[25] This experiment was complied with the known guidelines of animal ethics committee, which were established in accordance with the internationally accepted principles for laboratory animal use and care.

2.3. Experimental protocol

The rats were randomly divided equally into two groups:

Control group I (GI): It included 20 adult male rats, the animals of this group received 1 ml normal saline 0.9% intraperitoneally for 4 weeks.

Treated group II (GII): It included 20 rats, each animal received 50 mg/kg/day of tramadol intraperitoneally for 4 weeks.[17]

To prepare solution of the drug, 200 mg was dissolved in 20 ml of distilled water. Thus every 1 ml of the solution contained 10 mg of the drug. The animals were weighted and received the calculated dose of the drug according to their weight.

2.4. Histological study

All animals were anaesthetized by ether inhalation and perfused by normal saline. The brains were extracted from the skulls. For light microscopic study, the brains of 10 animals in each group were fixed in 10% formalin for 48 h. Tissues were dehydrated in ascending concentrations of alcohol, cleared in xylene and embedded in paraffin. Serial coronal sections, 5 μm in thickness were prepared and subjected to be studied by Einarson's Gallocyanin stain to demonstrate nuclei and nucleoli.[26] For electron microscopic study, the entorhinal cortex was dissected in 10 brains of each group. Tissues were fixed in phosphate buffered glutaraldehyde for 24 h and post fixed in 1% osmium tetroxide for one hour. Semithin sections (1 μm) were prepared and stained with toluidine blue. Ultrathin sections of 50 nm were cut by an ultra-microtome from selected areas, were contrasted with uranyl acetate and lead citrate[27] and were photographed with transmission electron microscope (Joel-JEM-100 CXII; Joel, Tokyo, Japan) in Assiut University Electron Microscopic Unit.

2.5. Morphometric study

Morphometric study was performed to determine the apoptotic index (AI)% of control and treated groups. The apoptotic index (AI)% was determined by counting a total of at least 1000 cells in layers II and III of entorhinal cortex per slide stained by toluidine blue. 10 non overlapping high-power fields (×400) were chosen randomly from each slide. AI% = [number of apoptotic cells/total number of calculated cells] × 100, is the percentage of apoptotic cells in 1000 cells.[28] Morphometric data were collected by using computer-based image analysis software (soft imaging system-An OPTIMAS version 6.2.1 program – Adept turnkey, Sydney, Australia).

2.6. Statistical study

All data were expressed as mean ± standard deviation (SD). Statistical analysis was carried out using (Graph Pad Software program – San Diego, California, USA). A Student's *t*-test was carried out for intergroup comparisons. $P > 0.05$, $P \leqslant 0.05$ and $P \leqslant 0.001$ were considered non-significant, significant and highly significant respectively.

3. Results

3.1. Histological results

3.1.1. Light microscopic results

3.1.1.1. Control group. The rat entorhinal cortex occupied the ventral-caudal part of the cerebral hemisphere and was bordered medially by the parasubiculum and laterally by the perirhinal cortex. Two main subdivisions of the entorhinal cortex were detected: lateral and medial entorhinal areas (Fig. 1).

In the control group, the structure of both lateral and medial entorhinal areas was found to be formed of the following layers; Layer I is poorly cellular (Figs. 2a, 2b, 3a, 3b, 4a and 4e) and Layer II contained cell islands of rounded cells. Their nuclei show prominent nucleoli (Figs. 2a, 2b, 2c, 3a, 3b, 4a and 4e). Layer III contained cells of various sizes and shapes but the medium pyramidal cells were the predominant type. The nuclei of these cells had prominent nucleoli (Figs. 2a, 2b, 2c, 3a, 3c, 4b and 4f). Layer IV (lamina dissecans) was a cell sparse layer (Figs. 2a, 2c, 3a and 3c). Layer V had large pyramidal neurons (Figs. 2a, 2d, 3a, 3c and 3d). Layer VI was characterized by the presence of cells of various sizes and shapes (Figs. 2a, 2d, 3a and 3d).

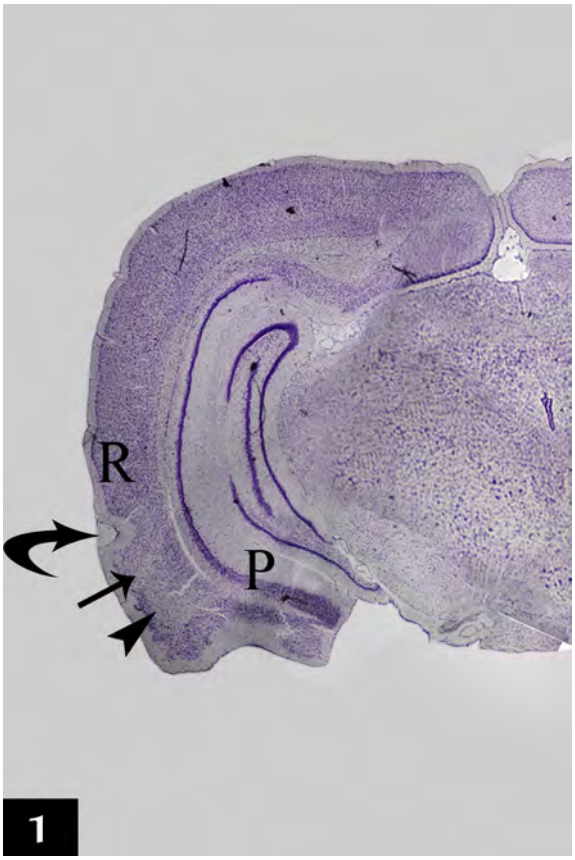

Figure 1 A photomicrograph of a coronal section in control adult rat cerebral hemisphere showing the location of the entorhinal cortex which is bordered medially by the parasubiculum (P) and laterally by the perirhinal cortex (R). Two main subdivisions of the entorhinal cortex were detected; the lateral (arrow) and the medial (arrow head) entorhinal areas. Curved arrow points to the rhinal fissure (RF) [Gallocyanine stain ×40].

3.1.1.2. Treated group. In the group of rats treated with tramadol, lateral entorhinal area showed neuronal cells disorganization in layers I, II, III, IV, V and VI (Fig. 2e). Degenerative vacuolization, intercellular edema, apoptotic cells characterized by neuronal shrinkage and chromatin condensation; margination and clumping, diffuse chromatolysis of nuclear chromatin and absence of nucleoli were detected in layers I, II, III, IV, V and VI (Figs. 2f, 2g, 2h, 4c and 4d). Multinuclear cells were present in layers IV (Fig. 2g). A dilated congested blood capillary was noticed in layer III (Fig. 2g). Absence of the nuclei was noticed in some neurons in layers II and III (Fig. 4c and 4d). In addition, dark neurons with hyperbasophilia were observed in layers I, II and III (Fig. 4c and 4d).

The degenerative changes observed in medial entorhinal area were more or less similar to those observed in lateral

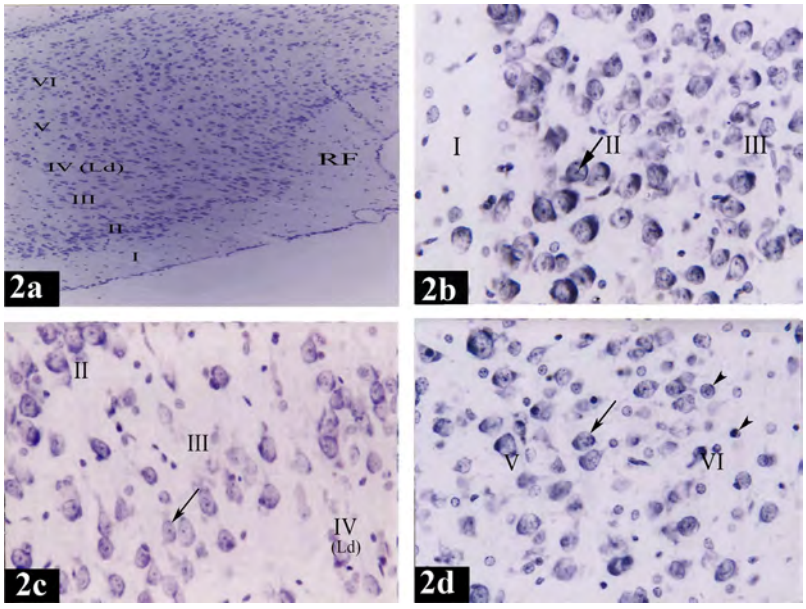

Plate 1 Photomicrographs of a coronal section in the lateral entorhinal area of control group (Figs. 2a, 2b, 2c and 2d). Fig. 2a shows neuronal cells organized in layers I, II, III, IV, V and VI. Ld points to lamina dissecans and RF points to the rhinal fissure. [Gallocyanine stain ×100]. Fig. 2b shows layer I (poorly cellular), layer II (contains cell islands of rounded cells), their nuclei have prominent nucleoli (arrow) and layer III (contains medium pyramidal cells) [Gallocyanine stain ×400]. Fig. 2c shows layer II (contains cell islands of rounded cells), layer III (contains medium pyramidal cells), prominent nucleoli in their nuclei (arrow) and layer IV. (Ld) points to lamina dissecans [Gallocyanine stain ×400]. Fig. 2d shows layer V [contains mainly large pyramidal cells (arrow)] and layer VI contains cells of various sizes and shapes (arrow heads) [Gallocyanine stain ×400].

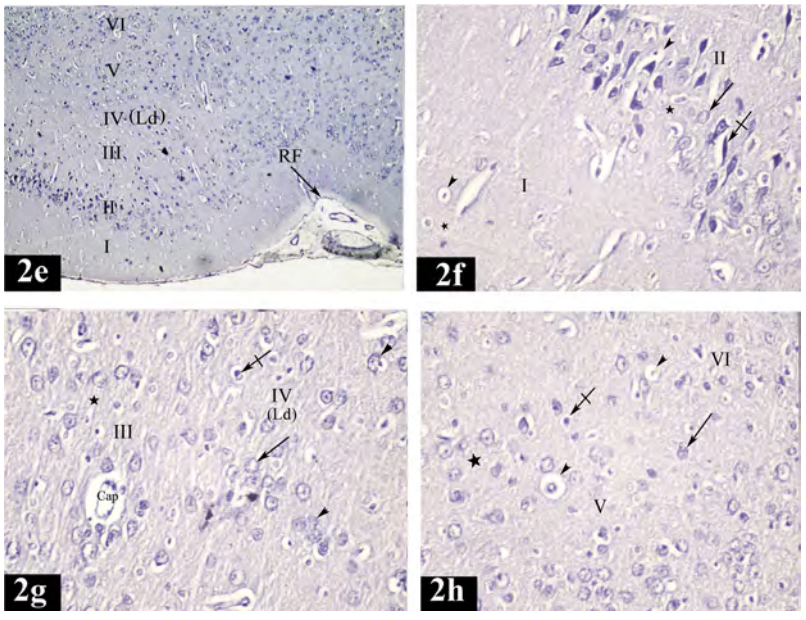

Plate 2 Photomicrographs of a coronal section in the lateral entorhinal area of treated group (Figs. 2e, 2f, 2g and 2h). Fig. 2e shows neuronal cells disorganization in layers I, II, III, IV, V and VI. (Ld) points to lamina dissecans and (RF) points to the rhinal fissure [Gallocyanine stain ×100]. Fig. 2f shows degenerative vacuolization (arrow heads) and intercellular edema (stars) in layers I and II. Layer II shows; apoptotic cells (crossed arrow) characterized by neuronal shrinkage and chromatin condensation, diffuse chromatolysis of nuclear chromatin and absence of nucleoli (arrow) [Gallocyanine stain ×400]. Fig. 2g shows apoptotic cells (crossed arrow), diffuse chromatolysis of nuclear chromatin and absence of nucleoli (arrow) and intercellular edema (star) in layers III and IV. Multinuclear cells are noticed in layer IV (arrowheads). Note a dilated congested blood capillary (Cap) in layer III. (Ld) points to lamina dissecans [Gallocyanine stain ×400]. Fig. 2h shows apoptotic cells (crossed arrow), extensive degenerative vacuolization (arrow heads), diffuse chromatolysis of nuclear chromatin and absence of nucleoli (arrow) and intercellular edema (star) in layers V and VI [Gallocyanine stain ×400].

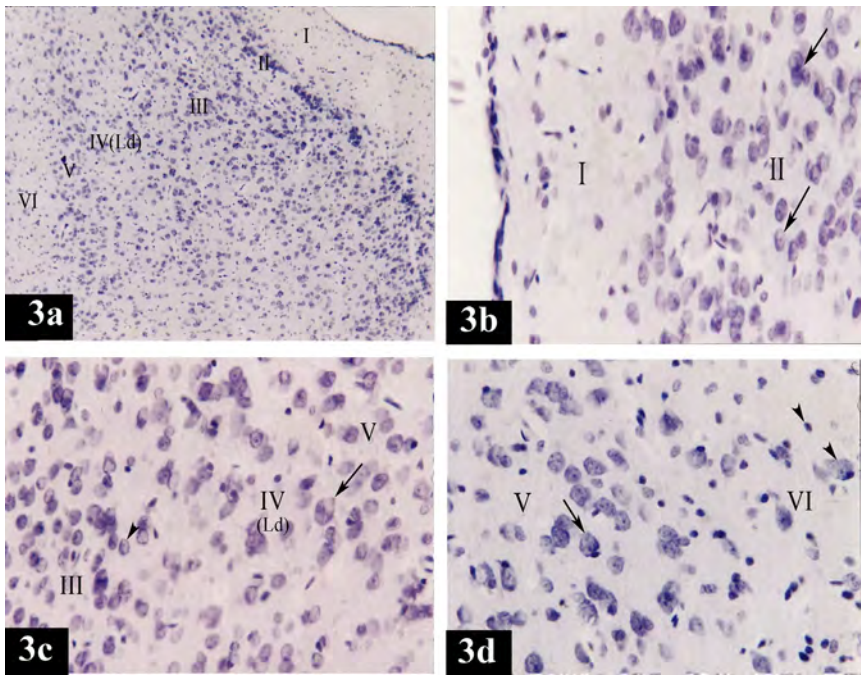

Plate 3 Photomicrographs of a coronal section in the medial entorhinal area of control group (Figs. 3a, 3b, 3c and 3d). Fig. 3a shows neuronal cells organized in layers I, II, III, IV, V and VI. (Ld) points to lamina dissecans [Gallocyanine stain × 100]. Fig. 3b shows layer I (poorly cellular) and layer II (contains cell islands of rounded cells). (Arrows) point to the prominent nucleoli in the nuclei [Gallocyanine stain ×400]. Fig. 3c shows layer III [contains medium pyramidal cells (arrow head)], layer IV, (Ld) points to lamina dissecans and layer V [contains mainly large pyramidal cells (arrow)] [Gallocyanine stain ×400]. Fig. 3d shows layer V [contains mainly large pyramidal cells (arrow)] and layer VI [contains cells of various sizes and shapes (arrow heads)] [Gallocyanine stain ×400].

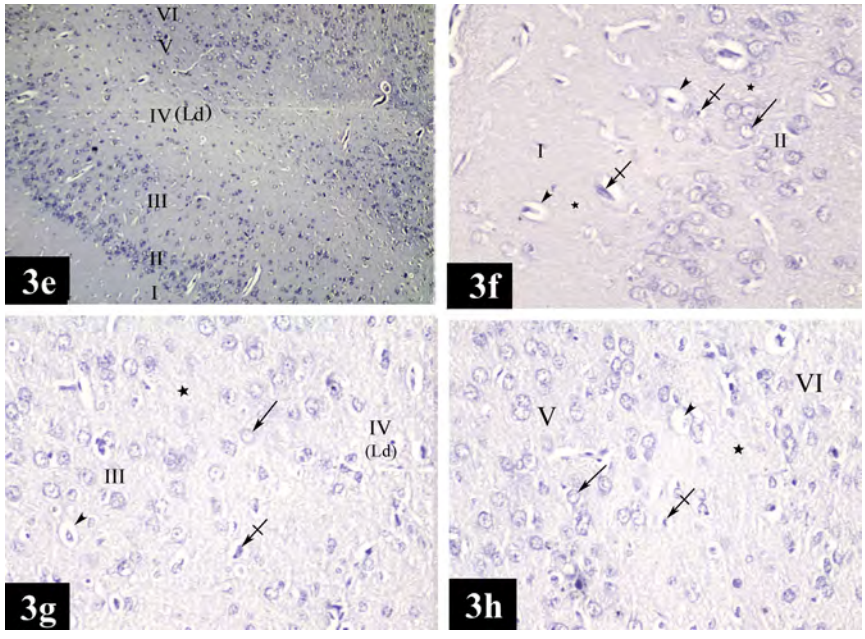

Plate 4 Photomicrographs of a coronal section in the medial entorhinal area of treated group (Figs. 3e, 3f, 3g and 3h). Fig. 3e shows neuronal cells disorganization in layers I, II, III, IV, V and VI. (Ld) points to lamina dissecans [Gallocyanine stain ×100]. Fig. 3f shows degenerative vacuolization (arrow heads), intercellular edema (stars) and apoptotic cells (crossed arrows) in layers I and II. Diffuse chromatolysis of nuclear chromatin and absence of nucleoli (arrow) could be noticed in layer II [Gallocyanine stain ×400]. Fig. 3g shows degenerative vacuolization (arrowhead), intercellular edema (star), apoptotic cells (crossed arrow), diffuse chromatolysis of nuclear chromatin and absence of nucleoli (arrow) in layers III and IV. (Ld) points to lamina dissecans [Gallocyanine stain × 400]. Fig. 3h shows apoptotic cells (crossed arrow), diffuse chromatolysis of nuclear chromatin and absence of nucleoli (arrow), degenerative vacuolization (arrow head) and intercellular edema (star) in layers V and VI [Gallocyanine stain ×400].

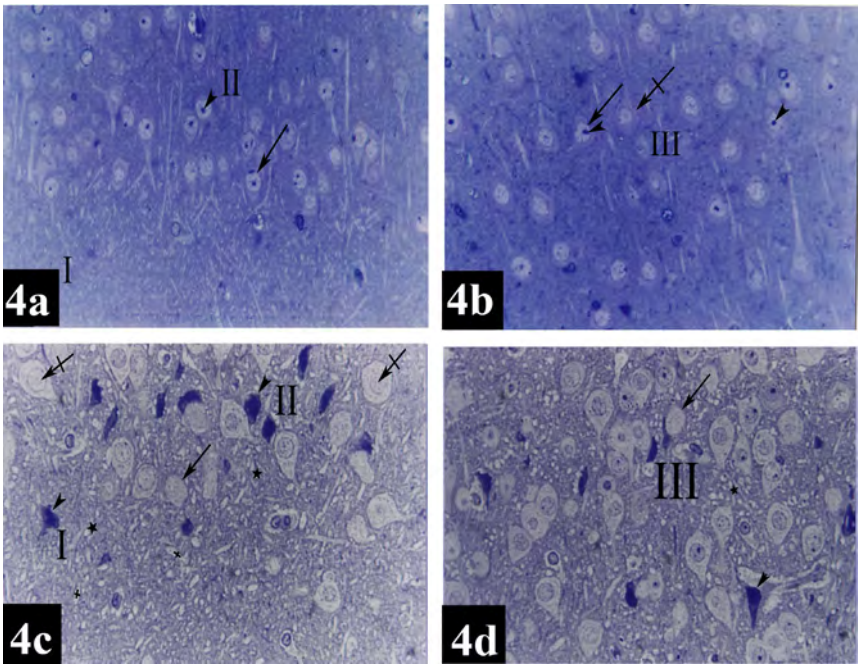

Plate 5 Photomicrographs of a coronal section in the lateral entorhinal area of control group (Figs. 4a and 4b) and treated group (Figs. 4c and 4d). Fig. 4a shows layers I (poorly cellular) and II (contains cell islands of rounded cells). Notice the prominent nucleoli (arrow head) in the nuclei (arrow) [Toluidine blue ×400]. Fig. 4b shows layer III contains medium pyramidal cells (crossed arrow). Their nuclei (arrow) have prominent nucleoli (arrow heads) [Toluidine blue ×400]. Fig. 4c shows dark neurons with hyperbasophilia (arrow heads), diffuse chromatolysis of nuclear chromatin and absence of nucleoli (crossed arrows), absence of nuclei (arrow), degenerative vacuolization (crosses) and intercellular edema (stars) in layers I and II [Toluidine blue ×400]. Fig. 4d shows dark neurons with hyperbasophilia (arrow head), absence of nuclei (arrow) and intercellular edema (star) in layer III [Toluidine blue ×400].

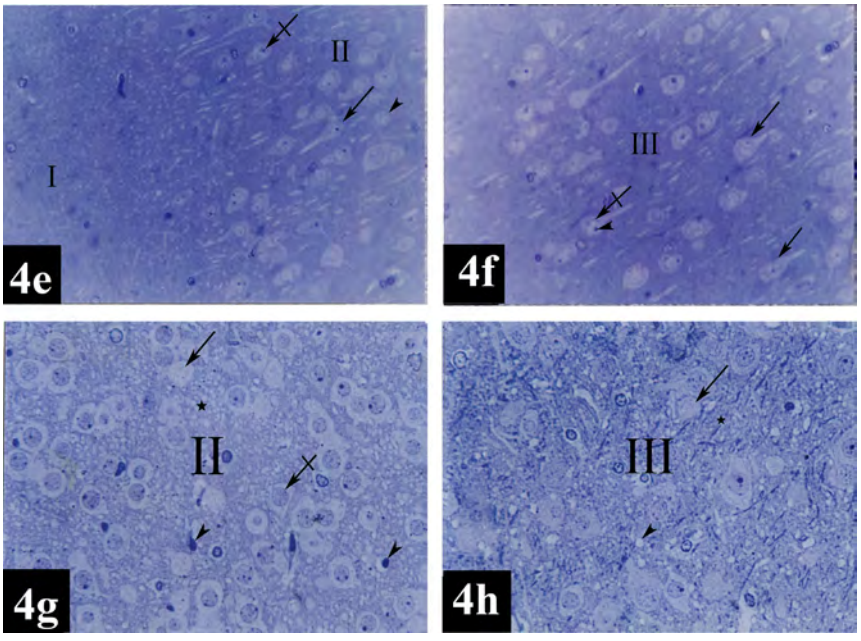

Plate 6 Photomicrographs of a coronal section in the medial entorhinal area of control group (Figs. 4e and 4f) and treated group (Figs. 4g and 4h). Fig. 4e shows layers I (poorly cellular) and II [contains mainly cell islands of rounded cells (arrow head)]. Notice the presence of prominent nucleoli (crossed arrow). Few pyramidal cells (arrow) can be detected within layer II [Toluidine blue ×400]. Fig. 4f shows layer III [contains medium pyramidal cells (arrows) and their nuclei (crossed arrow) with prominent nucleoli (arrow head)] [Toluidine blue ×400]. Fig. 4g shows apoptotic cells (arrowheads), diffuse chromatolysis of nuclear chromatin and absence of nucleoli (crossed arrow), absence of nuclei (arrow) and intercellular edema (star) in layer II [Toluidine blue ×400]. Fig. 4h shows absence of nuclei (arrow), intercellular edema (star) and degenerative vacuolization (arrow head) in layer III [Toluidine blue ×400].

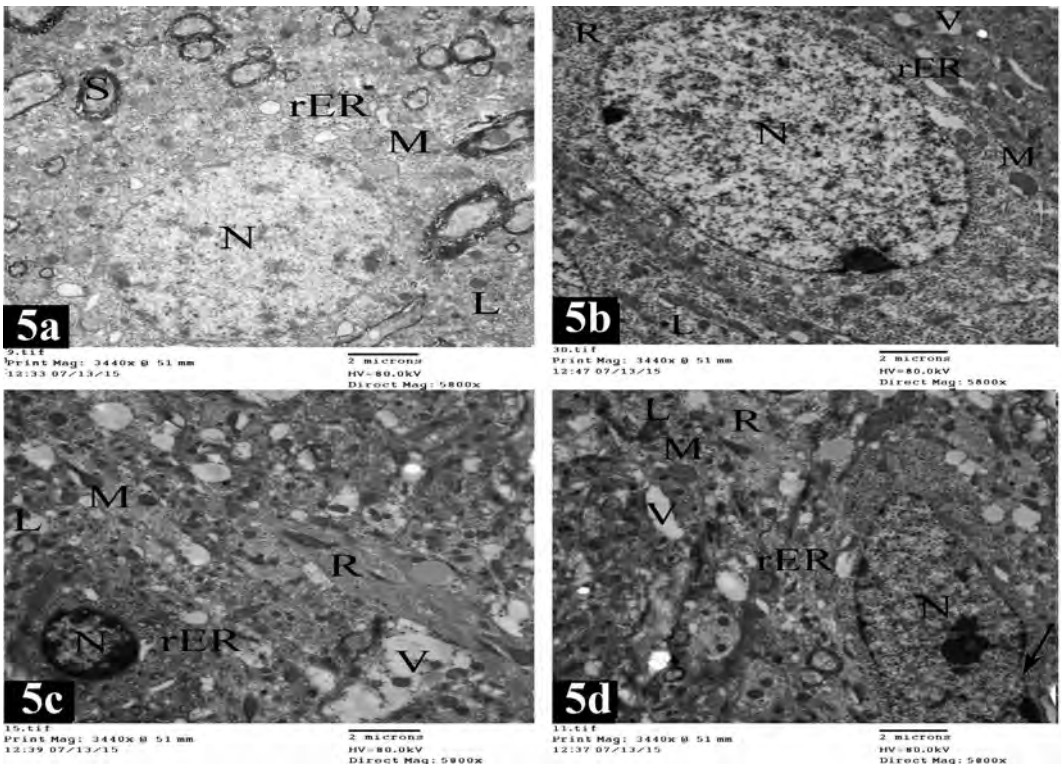

Plate 7 Electron micrographs of lateral entorhinal area of control group (Figs. 5a and 5b) and treated group (Figs. 5c and 5d). Fig. 5a shows a granular cell in layer II. The cell has rounded nucleus (N) with fine granular chromatin. The cytoplasm is rich with rough endoplasmic reticulum cisternae (rER), numerous mitochondria (M) and lysosomes (L). Notice the presence of nerve fibers surrounded with myelin sheaths (S) [×5800]. Fig. 5b shows a pyramidal cell in layer III. It has oval nucleus (N) with electron dense heterochromatin. The cytoplasm contains rough endoplasmic reticulum cisternae (rER), mitochondria (M), numerous free ribosomes (R), lysosomes (L) and few vacuoles (V) [×5800]. Fig. 5c shows a granular cell in layer II. The cell shows shrinkage rounded nucleus (N) and chromatin condensation; margination, and clumping with extensive electron dense heterochromatin. The cytoplasm contains free ribosomes (R), distorted rough endoplasmic reticulum cisternae (rER), many degenerative vacuoles (V), lysosomes (L) and disorganized mitochondria (M) [×5800]. Fig. 5d shows a pyramidal cell in layer III. The cell has oval nucleus (N), chromatin condensation; margination and clumping with electron dense heterochromatin. (Arrow) points to irregularity of nuclear envelope. The cytoplasm contains degenerative vacuoles (V), lysosomes (L), free ribosomes (R), mitochondria swollen (M) and distorted rough endoplasmic reticulum cisternae (rER) [×5800].

entorhinal area. Layers I, II, III, IV, V and VI were characterized by neuronal cells disorganization (Fig. 3e). Intercellular edema, apoptotic cells characterized by neuronal shrinkage and chromatin condensation; margination and clumping, degenerative vacuolization, some cells with diffuse chromatolysis of nuclear chromatin and absence of nucleoli were detected in layers I, II, III, IV, V and VI (Figs. 3f, 3g, 3h, 4g and 4h). Some neurons presented with absence of their nuclei (Figs. 4g and 4h).

3.1.2. Electron microscopic results

3.1.2.1. Control group. Electron microscopic examination of the granular cells of layer II in lateral entorhinal area revealed that the cells had rounded nuclei with fine granular chromatin. Their cytoplasm contained rough endoplasmic reticulum cisternae, numerous mitochondria and lysosomes. Nerve fibers surrounded with myelin sheaths were present (Fig. 5a).

The pyramidal cells of layer III in the lateral entorhinal area had oval nuclei with electron dense heterochromatin. Their cytoplasm contained abundant amount of rough endoplasmic reticulum cisternae, mitochondria, numerous free ribosomes, lysosomes and few vacuoles (Fig. 5b).

Electron microscopic examination of medial entorhinal area revealed the presence of two types of cells. The granular cells of layer II had rounded nuclei with electron dense heterochromatin. Their cytoplasm showed rough endoplasmic reticulum, mitochondria and lysosomes. Nerve fibers surrounded with myelin sheaths could be observed (Fig. 5e). Pyramidal cells of layer III had oval nuclei with fine granular chromatin. Their cytoplasm was rich with rough endoplasmic reticulum, mitochondria and free ribosomes. Nerve fibers surrounded with myelin sheaths were noticed (Fig. 5f).

3.1.2.2. Treated group. In treated rats, the granular apoptotic cells in the lateral entorhinal area showed shrinkage rounded nuclei and chromatin condensation; margination and clumping with extensive electron dense heterochromatin. Their cytoplasm contained free ribosomes, distorted rough endoplasmic reticulum, many degenerative vacuoles and lysosomes. In addition, disorganized mitochondria were observed (Fig. 5c).

The pyramidal apoptotic cells in the lateral entorhinal area showed oval nuclei, chromatin condensation; margination and

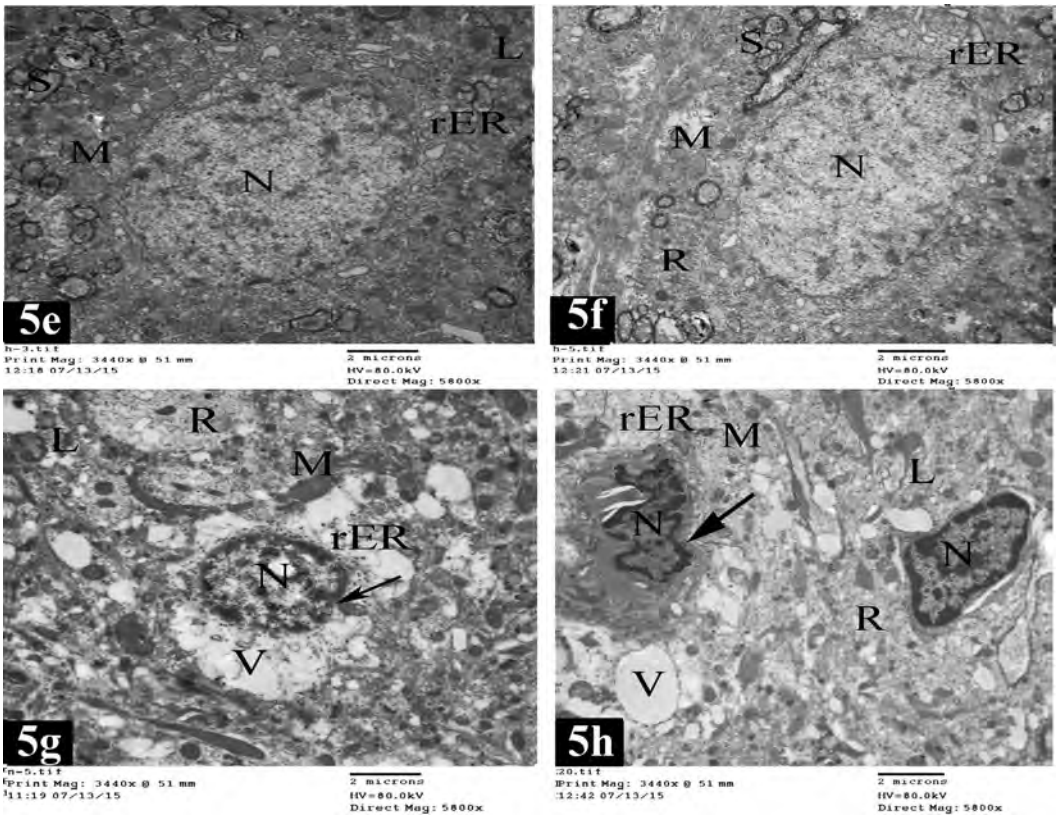

Plate 8 Electron micrographs of medial entorhinal area of control group (Figs. 5e and 5f) and treated group (Figs. 5g and 5h). Fig. 5e shows a granular cell in layer II. The cell contains rounded nucleus (N) with electron dense heterochromatin. The cytoplasm contains rough endoplasmic reticulum cisternae (rER), mitochondria (M) and lysosomes (L). Notice the presence of nerve fibers surrounded with myelin sheaths (S) [×5800]. Fig. 5f shows a pyramidal cell in layer III with oval nucleus (N) and fine granular chromatin. The cytoplasm contains rough endoplasmic reticulum cisternae (rER), mitochondria (M) and free ribosomes (R). Nerve fibers surrounded with myelin sheaths (S) are present [×5800]. Fig. 5g shows a granular cell in layer II. It has shrinkage rounded nucleus (N) and chromatin condensation; margination and clumping with electron dense heterochromatin. (Arrow) points to irregularity of nuclear envelope. The cytoplasm contains numerous degenerative vacuoles (V), lysosomes (L), free ribosomes (R), mitochondria swollen (M) and distorted rough endoplasmic reticulum cisternae (rER) [×5800]. Fig. 5h shows pyramidal cells in layer III. The cells have shrinkage oval nuclei (N) and chromatin condensation; margination and clumping with electron dense heterochromatin. (Arrow) points to marked irregularity of nuclear envelope. The cytoplasm shows numerous degenerative vacuoles (V), lysosomes (L), free ribosomes (R), damaged mitochondria (M) and distorted rough endoplasmic reticulum cisternae (rER) [×5800].

clumping, with electron dense heterochromatin. Irregularity of nuclear envelope could be observed. Their cytoplasm had many degenerative vacuoles, lysosomes and free ribosomes. Mitochondria swollen and distorted rough endoplasmic reticulum were present (Fig. 5d).

Electron microscopic examination of medial entorhinal area showed obvious degenerative changes. The granular apoptotic cells had shrinkage rounded nuclei, chromatin condensation; margination, and clumping with electron dense heterochromatin and irregularity of nuclear envelope. Many degenerative vacuoles, lysosomes, free ribosomes, mitochondria swollen and distorted rough endoplasmic reticulum were present in the cytoplasm (Fig. 5g).

The pyramidal apoptotic cells had shrinkage oval nuclei, chromatin condensation; margination, and clumping, with electron dense heterochromatin and irregularity of nuclear envelope. Many degenerative vacuoles, lysosomes, free ribosomes, damaged mitochondria and distorted rough endoplasmic reticulum could be detected in the cytoplasm (Fig. 5h).

3.2. Morphometric and statistical results

The mean value ± SD (standard deviation) of the apoptotic index% in the treated group (GII) was 2.63 ± 26.08 which showed high significant increase ($P \leqslant 0.001$) as compared to the control group (GI) where the apoptotic index % was 0.97 ± 1.20 (Table 1 and Histogram 1).

Table 1 The mean value ± SD of the apoptotic index % in GI and GII.

Groups	Mean ± SD
Control (GI)	1.20 ± 0.97
Treated (GII)	26.08 ± 2.63
P (I versus II)	0.0001[a]

Data are presented as the mean values ± SD (standard deviation) in GI and GII.

[a] $P \leqslant 0.001$ versus control (highly significant).

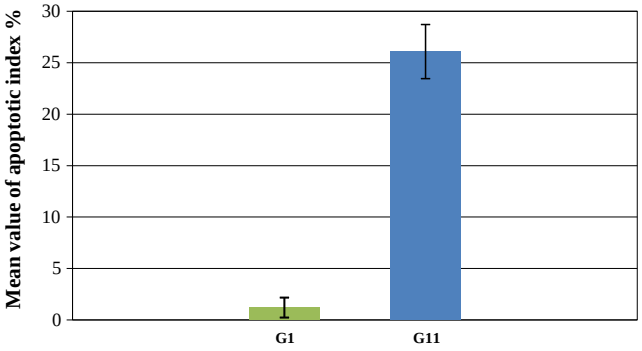

Histogram 1 Mean values ± SD (standard deviation) of apoptotic index % of control (GI) and treated (GII) groups. $P \leqslant 0.001$ versus control (highly significant).

4. Discussion

The current study aimed to assess the deleterious effects of tramadol on the entorhinal cortex of the adult male albino rats. Tramadol belongs to the synthetic opioid analgesic that is commonly prescribed for moderate to severe pain. It has been called an "atypical" opioid because both an opioid component and a nonopioid component have been demonstrated in its mechanism of action.[29] The brain is particularly susceptible to oxidative damage due to its high levels of oxygen consumption, increased levels of polyunsaturated fatty acids and relatively low levels of antioxidants.[30]

The present study revealed that tramadol resulted in obvious degenerative changes in both lateral and medial entorhinal areas. These observations were in agreement with the results of the previous studies that reported the oxidative stress induced by the tramadol in brain.[31–34] The tramadol not only induced oxidative stress in brain but also was associated with significant decrease in brain non-enzymatic antioxidant, intracellular reduced glutathione level and enzymatic antioxidant and glutathione peroxidase activity.[35] Moreover, it has been reported that oxidative modifications resulted in a loss of function and lowering of enzyme activity.[36] In addition a long-term effect of tramadol on neuronal glucose metabolism and insulin signaling pathway in the cerebral cortex consequently leads to development of oxidative stress.[37]

In this study, light microscopic examination of the lateral and medial entorhinal areas showed neuronal cells disorganization, intercellular edema, apoptotic cells characterized by neuronal shrinkage and chromatin condensation, degenerative vacuolization and dark neurons with hyperbasophilia. Dilated congested blood vessels were also detected. In harmony with the present results some investigators reported the presence of congested sub meningeal blood vessels and neuronal degeneration following tramadol administration.[38] These findings coincided with Liu et al.[39]. They stated that the multiple effects of opioids on neuronal structure (cytoskeleton) have been regarded as the markers of neuronal damage due to long term use of morphine and other opioids. They also found that the apoptotic cells were present with cytoplasmic contraction, reduction in cell volume and nuclear chromatin condensation.

In this work, electron microscopic examination revealed the presence of apoptotic pyramidal and granular cells in both lateral and medial entorhinal areas. These apoptotic cells showed shrinkage of nuclei, irregularity of the nuclear envelope, chromatin condensation, mitochondria swollen, degenerative vacuolation and distorted rough endoplasmic reticulum. These histological findings were confirmed by the morphometric and statistical results as apoptotic index showed high significant increase in the treated group in comparison with the control group. Mohamed et al.[40] noticed that tramadol administration resulted in loss of pyramidal cells shape, perivascular space increased with hemorrhage, and disrupted ependyma and choroid plexus became hypertrophied. The chronic use of morphine and/or tramadol in increasing doses was found to cause neuronal degeneration and apoptosis in the rat brain, which probably contributed to cerebral dysfunction.[41]

In the present study, the degenerative vacuolation could be attributed to the damaged cell organoid from exposure to free radicals.[42,43] The observed mitochondrial changes might be considered as early manifestation of apoptosis and an adaptive process to unfavorable environments as excess exposure of the cell to free radicals at the level of intracellular organelles. These suggestions might be confirmed by the successful suppression of these changes by free radical scavengers.[44] It has been reported that Complexes I, III, and IV of electron transfer chain (ETC) in mitochondria were found to be inhibited by tramadol at high doses. Inhibition of complex III resulted in the generation of reactive oxygen species as a consequence of the intrinsic characteristics of the electron transfer process to this complex from reduced ubiquinone.[40,45]

The toxic effects of tramadol at the cellular level could be explained by increasing lipid peroxidation that could be used as a marker of the reactive oxygen species (ROS)-induced cell damages.[32] Moreover, it has been found that lipid peroxidation was significantly increased in chronic heroin users.[46] These data were confirmed by the results of previous studies done by Zhang et al.[47] and Atici et al.[48] as they demonstrated that treatment with morphine and tramadol yielded an increased malondialdehyde (MDA) level, which suggested an increased lipid peroxidation. In addition, they observed a decrease in the level of reduced glutathione in the isolated rat hepatocytes in the case of incubation with different opioids concentration (yielding cell death) and they also noticed a lowered content of reduced glutathione and activities of catalase, superoxide dismutase and glutathione peroxidase.

5. Conclusion

The results of the present study provided evidence that tramadol intake exerted a neurotoxic effect on the structure of both lateral and medial entorhinal areas. So tramadol abuse should be avoided without medical description. Further investigations are needed for more comparison and interpretation.

Conflict of interest

There is no conflict of interest to declare.

References

1. World Health Organization. *Cancer pain relief: with a guide to opioid availability*. Geneva: World Health Organization; 1996. p. 1–63.

2. Barkin RL. Extended-release tramadol (ULTRAM ER): a pharmacotherapeutic, pharmacokinetic and pharmacodynamic focus on effectiveness and safety in patients with chronic/persistent pain. *Am J Ther* 2008;**15**(2):157–66.
3. Keating GM. Tramadol sustained-release capsules. *Drugs* 2006;**66**(2):223–30.
4. Radbruch L, Glaeske G, Grond S, Munchberg F, Scherbaum N, Storz E, et al. Topical review on the abuse and misuse potential of tramadol and tilidine in Germany. *Subst Abus* 2013;**34**(3):313–20.
5. Soyka M, Backmundm M, Hasemann S. Tramadol use and dependence in chronic noncancer pain patients. *Pharmacopsychiatry* 2004;**37**(4):191–2.
6. McKeon GP, Pacharinsak C, Long CT, Howaed AM, Jampachaisri K, Yeomans DC, et al. Analgesic effects of tramadol, tramadol – gabapentin and buprenorphine in an incisional model of pain in rats (Rattus norvegicus). *J Am Assoc Lab Anim Sci* 2011;**50**(2):192–7.
7. Barsotti CE, Mycyk MB, Reyes J. Withdrawal syndrome from tramadol hydrochloride. *Am J Emerg Med* 2003;**21**(1):87–8.
8. Angela ND, George EB, Ryan KL, Eric CS. Discriminative stimulus effects of tramadol in humans. *J Pharmacol Exp Ther* 2011;**338**(1):255–62.
9. Barbera N, Fisichella M, Bosco A, Indorato F, Spadaro G, Romano GA. Suicidal poisoning due to tramadol. A metabolic approach to death investigation. *J Forensic Leg Med* 2013;**20**(5):555–8.
10. De Backer B, Renardy F, Denooz R, Charlier C. Quantification in postmortem blood and identification in urine of tramadol and its two main metabolites in two cases of lethal tramadol intoxication. *J Anal Toxicol* 2010;**34**(9):599–604.
11. De Decker K, Cordonnier J, Jacobs W, Coucke V, Schepens P, Jorens PG. Fatal intoxication due to tramadol alone: case report and review of the literature. *Forensic Sci Int* 2008;**175**(1):79–82.
12. Mannocchi G, Napoleoni F, Napoletano S, Pantano F, Santoni R, Tittarelli R, et al. Fatal self-administration of tramadol and propofol: a case report. *J Forensic Leg Med* 2013;**20**(6):715–9.
13. Tjaderborn M, Jonsson AK, Hagg S, Ahlner J. Fatal unintentional intoxications with tramadol during 1995–2005. *Forensic Sci* 2007;**173**(2–3):107–11.
14. Nayyar N. Serotonin syndrome associated with sertraline, trazodone and tramadol abuse. *Indian J Psychiatry* 2009;**51**(1):68.
15. Sanaei-Zadeh H. Serotonin syndrome induced by tramadol intoxication in an 8-month-old infant. *Pediatr Neurol* 2011;**44**(1):72–4.
16. Tashakori A, Afshari R. Tramadol overdose as a cause of serotonin syndrome: a case series. *Clin Toxicol (Phila)* 2010;**48**(4):337–41.
17. Matthiesen T, Wohrmann T, Coogan TP, Uragg H. The experimental toxicology of tramadol: an overview. *Toxicol Lett* 1998;**95**(1):63–71.
18. Canto CB, Wouterlood FG, Witter MP. What does the anatomical organization of the entorhinal cortex tell us? *Neural Plas* 2008;**1238**:1243.
19. Moser EI, Witter MP, Moser MB. Entorhinal cortex. In: Shepherd S, Grillner S, editors. *Handbook of brain microcircuits*. Oxford (UK): Oxford Univ. Press; 2010. p. 175–92.
20. Braak H, Braak E. On areas of transition between entorhinal allocortex and temporal isocortex in the human brain. Normal morphology and lamina-specific pathology in Alzheimer's disease. *Acta Neuropathol (Berl)* 1985;**68**:325–32.
21. DeToledo-Morrell L, Stoub TR, Bulgakova M, Wilson RS, Bennett DA, Leurgans S, et al. MRI-derived entorhinal volume is a good predictor of conversion from MCI to AD. *Neurobiol Aging* 2004;**25**:1197–203.
22. Du F, Whetsell WO, Abou-Khalil B, Blumenkopf B, Lothman R, Schwarcz R. Preferential neuronal loss in layer III of the entorhinal cortex in patients with temporal lobe epilepsy. *Epilepsy Res* 1993;**16**:223–33.
23. Arnold SE. Cellular and molecular neuropathology of the parahippocampal region in schizophrenia. *Ann N Y Acad Sci* 2000;**911**:275–92.
24. Baiano M, Perlini C, Rambaldelli G, Cerini R, Dusi N, Bellani M, et al. Decreased entorhinal cortex volumes in schizophrenia. *Schizophr Res* 2008;**102**:171–80.
25. National Research Council (NRC) Committee on Animal Nutrition. Nutrient requirement of laboratory animals, vol. 31. No. 10, 3rd revised ed. Washington (DC): National Academy of Science, National Research Council; 1978.
26. Marilyn G, John DB. *Theory and practice of histological techniques*. 6th ed. Churchill Livingstone; 2008. p. 228.
27. Hayat MA. *Principles and techniques of electron microscopy: biological applications*. 4th ed. Edinburgh (UK): Cambridge University Press; 2000. p. 37–59.
28. Fatma MG, Hanaa AK, Ayman ZE, Ahmed NH. Effect of chronic usage of tramadol on motor cerebral cortex and testicular tissues of adult male albino rats and the effect of its withdrawal: histological, immunohistochemical and biochemical study. *Int J Clin Exp Pathol* 2014;**7**(11):7323–41.
29. Norma CM, Eva GT Ma, Miguel H, Xochitl TM, Irene DR. Tramadol and tramadol caffeine synergism in the rat formalin test are mediated by central opioid and serotonergic mechanisms. *J Biol Med Res Int* 2015, 686424686433.
30. Butterfield DA, Castegna A, Lauderback CM, Drake J. Evidence that amyloid beta-peptide-induced lipid peroxidation and its sequelae in Alzheimer's disease brain contribute to neuronal death. *Neurobiol Aging* 2002;**23**:655–64.
31. El-Gaafarawi II. Biochemical toxicity induced by tramadol administration in male rats. *Egypt J Hosp Med* 2006;**23**:353–62.
32. Popovic M, Janicijevic-Hudomal S, Kaurinovic B, Rasic J, Trivic M, Vojnović M. Antioxidant effects of some drugs on immobilization stress combined with cold restraint stress. *Molecules* 2009;**14**:4505–16.
33. Rabei HM. The immunological and histopathological changes of tramadol, tramadol/acetaminophen and acetaminophen in male albino rats "Comparative study". *Egypt J Hosp Med* 2011;**45**:477–503.
34. Costa PF, Nunes N, Belmonte EA, Moro JV, Lopes PCF. Hematologic changes in propofol-anesthetized dogs with or without tramadol administration. *Arq Bras Med Vet Zootec* 2013;**65**:1306–12.
35. Abdel-Zaher AO, Abdel-Rahman MS, ELwasei FM. Protective effect of Nigella sativa oil against tramadol-induced tolerance and dependence in mice: role of nitric oxide and oxidative stress. *Neuro Toxicol* 2011;**32**:725–33.
36. Butterfield DA, Reed T, Newman SF, Sultana R. Roles of amyloid beta-peptide-associated oxidative stress and brain protein modifications in the pathogenesis of Alzheimer's disease and mild cognitive impairment. *Free Radic Biol Med* 2007;**43**:658–77.
37. Kanter M. Nigella sativa and derived thymoquinone prevent hippocampal neurodegeneration after chronic toluene exposure in rats. *Neurochem Res* 2008;**33**:579–88.
38. Abou El Fatoh MF, Farag M, Sayed AE, Kamel MA, Abdel-Hamid N, Hussein M, et al. Some biochemical, neurochemical, pharmacotoxicological and histopathological alterations induced by long-term administration of tramadol in male rats. *Int J Pharm Sci* 2014;**4**:565–71.
39. Liu LW, Lu J, Wang XH, Fu SK, Li Q, Lin FQ. Neuronal apoptosis in morphine addiction and its molecular mechanism. *Int J Clin Exp Med* 2013;**6**:540–5.
40. Mohamed TM, Abdel Ghaffar HM, El Husseiny RM. Effects of tramadol, clonazepam and their combination on brain mitochondrial complexes. *Toxicol Ind Health* 2015;**31**(12):1325–33.
41. Atici S, Cinel L, Cinel I, Doruk N, Aktekin M, Akca A, et al. Opioid neurotoxicity: comparison of morphine and tramadol in an experimental rat model. *Int J Neurosci* 2004;**114**:1001–11.

42. Zarnescu O, Brehar FM, Chivu M, Ciurea AV. Immunohistochemical localization of caspase-3, caspase-9 and Bax in U87 glioblastoma xenografts. *J Mol Histol* 2008;**39**:561–9.
43. Brown DM, Donaldson K, Borm PJ, Schins RP, Dehnhardt M, Gilmour P, et al. Calcium and ROS-mediated activation of transcription factors and TNFalpha cytokine gene expression in macrophages exposed to ultrafine particles. *Am J Physiol Lung Cell Mol Physiol* 2004;**286**:344–53.
44. Wakabayashi T. Mega mitochondria formation-physiology and pathology. *J Cell Mol Med* 2002;**6**:497–538.
45. Lemarie A, Grimm S. Mutations in the heme b-binding residue of SDHC inhibit assembly of respiratory chain complex II in mammalian cells. *Mitochondrion* 2009;**9**:254–60.
46. Panchenko LF, Pirozhkov SV, Nadezhdin AV, Baronets VI, Usmanova NN. Lipid peroxidation, peroxyl radical scavenging system of plasma and liver and heart pathology in adolescence heroin users. *Vopr Med Khim* 1999;**45**:501–6.
47. Zhang YT, Zheng QS, Pan J, Zheng RL. Oxidative damage of biomolecules in mouse liver induced by morphine and protected by antioxidants. *Basic Clin Pharmacol Toxicol* 2004;**95**:53–8.
48. Atici S, Cinel I, Cinel L, Doruk N, Eskandari G, Oral U. Liver and kidney toxicity in chronic use of opioids: an experimental long term treatment model. *J Biosci* 2005;**30**:245–52.